

1

1

Counterexamples of Boltzmann's equation

C. Y. Chen

Department of Physics, Beijing University of Aeronautics
and Astronautics, Beijing, 100083, P. R. China

March 23, 2024

PACS 51.10.+y. Kinetic and transport theory of gases

Abstract

To test kinetic theories, simple and practical setups are proposed. It turns out that these setups cannot be treated by Boltzmann's equation. An alternative method, called the path-integral approach, is then employed and a number of ready-for-verification results are obtained.

1 Introduction

One of the fundamental mysteries in statistical physics is that the derivation of Boltzmann's equation explicitly resorts to the time reversibility of Newtonian mechanics whereas the derived equation seems to offer a plausible account for time irreversibility. This logic puzzle has been around us for more than a hundred years and a large number of interpretations motivated to clear up the issue kept on appearing in the literature.

Without much attention received, we took another direction and questioned the mathematical and physical validity of Boltzmann's equation [1]. In this paper, we concern ourselves with proposing simple and practical setups, in which Boltzmann's equation, or any other alternatives, can be put to computational and/or experimental tests.

Two types of collisions get involved: particle-to-boundary collisions and particle-to-particle collisions. In view of that every particle can be thought

Email: cychen@buaa.edu.cn

of as a particle scattered by boundaries or by other particles, the generality of this discussion is rather obvious.

It turns out that for the proposed setups Boltzmann's equation yields either incomputable or unreasonable results. With that in mind, an alternative method, called the path-integral approach, is employed and a number of ready-for-verification results are derived.

If interested enough, readers may devise their own ways to prove or disprove every conclusion offered by this paper.

2 Two setups

To test Boltzmann's theory, as well as its alternatives, we advance the following two setups, which can be easily realized in real or computer-simulated experiments.

Setup 1: Referring to Fig. 1, consider a parallel beam whose distribution is

$$f^0(v^0) = n^0 g(v_x^0) \delta(v_y^0 - 0) \delta(v_z^0 - 0); \quad (1)$$

where $v_x^0 > 0$ and $g(v_x^0)$ is a nonnegative normalized function; and let it hit a solid boundary of finite size. It is obvious that the distribution given above is quite normal; for instance the relationship

$$\int_{-\infty}^{\infty} \int_{-\infty}^{\infty} \int_{-\infty}^{\infty} f^0(v^0) dv_x^0 dv_y^0 dv_z^0 = n^0 \quad (2)$$

exists, where n^0 is the ordinary particle density of the beam.

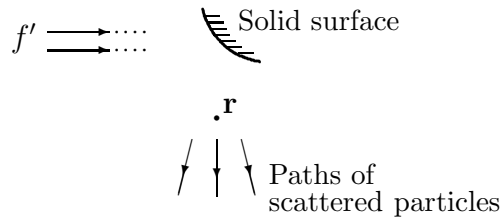


Figure 1: Particles of a beam collide with a solid surface.

Setup 2: Consider two head-on parallel beams shown in Fig. 2. Beam 0 which moves rightwards is described also by the distribution function

(1); and beam 1 is described by

$$f_1^0(v_1^0) = n_1^0 g_1(v_{1x}^0) \delta(v_{1y}^0 - 0) \delta(v_{1z}^0 - 0); \quad (3)$$

where $v_{1x}^0 < 0$ and $g_1(v_{1x}^0)$ is again a nonnegative normalized function. Though having the same mass, the particles belonging to beam 0 and beam 1 (sometimes referred to as type 0 and type 1 particles respectively) are considered to be distinguishable in this paper. The transverse sections of the two beams are finite, say, shaped like circular ones.

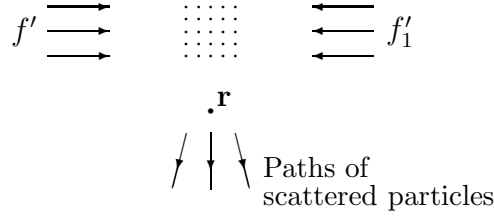


Figure 2: Two beams collide. The collision region is highlighted by dots.

To make the discussion less complicated, we shall ignore any external forces and disregard particles that suffer collisions twice or more (letting be small and/or the gas be dilute). With the assumption that all colliding parallel beams are produced by stable external sources, the two setups are considered to be time-independent.

3 Application of Boltzmann's equation

According to the standard theory [3, 4], in a spatial region where collisions are ignorable, the distribution function, denoted by $f(t; r; v)$ with r representing the position $(x; y; z)$, satisfies the collisionless Boltzmann equation

$$\frac{\partial f}{\partial t} + v \frac{\partial f}{\partial r} + \frac{F}{m} \frac{\partial f}{\partial v} = 0; \quad (4)$$

in which F stands for the external force acting on the particles. In a region where collisions cannot be ignored, the regular Boltzmann equation reads

$$\frac{\partial f}{\partial t} + v \frac{\partial f}{\partial r} + \frac{F}{m} \frac{\partial f}{\partial v} = \int_{v_1}^Z \int_{-c}^Z 2u (f^0 f_1^0 - f f_1) (-c) d_c dv_1; \quad (5)$$

where $f^0(v^0)$ and $f_1^0(v_1^0)$ represent the particles that collide to make $f(v)$ increase, $f_1(v_1)$ represents the particles that collide with $f(v)$ to make $f(v)$ decrease, $(2u)$ is the relative speed of the colliding particles, Ω_c is the solid angle formed by the initial relative velocity and final relative velocity, and (σ_c) is the cross section in terms of Ω_c .

In the following two subsections, we shall apply (4) and (5) to the setups given in Section 2.

3.1 Application to setup 1

It is trivial to see how the parallel beam illustrated in Fig. 1 obeys the collisionless Boltzmann equation (4). Noting that the beam is stationary and there is no external force, namely $\partial f^0/\partial t = 0$ and $F = 0$, we obtain from (4)

$$v^0 \frac{\partial f^0(v^0)}{\partial r} = 0 \quad \text{or} \quad \frac{\partial f^0}{\partial r_{\text{path}}} = 0; \quad (6)$$

which is indeed satisfied by (1). For later use, it should be mentioned that (6) characterizes parallel beams.

We now turn our attention to the particles scattered by the solid surface, whose distribution function will be denoted by $f(t; r; v)$. Again, due to the existence of $\partial f/\partial t = 0$ and $F = 0$, the collisionless Boltzmann equation (4) yields

$$\frac{\partial f}{\partial r_{\text{path}}} = 0 \quad \text{or} \quad f|_{\text{path}} = \text{Constant}; \quad (7)$$

The deduction of (7) is simple, but difficult things arise. As Fig. 1 has intuitively shown, the scattered particles will not form a parallel beam and their density will in general decrease along the paths (which can be easily verified in experiments), but according to (7) they seem to form a parallel beam and their density seems to keep constant along any path of the scattered particles. If we wish to adopt (7), for whatever reason, we shall encounter great difficulty in interpreting it, let alone verify it in experiments.

3.2 Application to setup 2

In this subsection, $f(t; r; v)$ denotes the distribution function of scattered beam 0 particles shown in Fig. 2.

Firstly, we examine the situation outside the collision region. Again, the collisionless Boltzmann equation gives rise to

$$v \frac{\partial f}{\partial r} = 0 \quad \text{or} \quad f|_{\text{path}} = \text{Constant}; \quad (8)$$

Some of the problems related to (8) have been discussed, of which one is that the density of the scattered particles will decrease along the paths, while (8) suggests otherwise.

Then, we wish to find out what happens inside the collision region, where the regular Boltzmann equation (5) is supposed to hold.

The second term on the right side of (5) takes the form

$$\int_{v_1} \int_{c_c} 2uf(v)f_1(v_1) \delta(c) d_c dv_1: \quad (9)$$

It is trivial to find that this integral is computable. However, since \emptyset is associated with particles that suffer collisions two times or more (itself stands for particles produced by collisions), we shall consider it no more.

After (9) is omitted, (5) becomes, by virtue of $\partial f / \partial t = 0$ and $F = 0$,

$$v \frac{\partial f}{\partial r} = \int_{v_1} \int_{c_c} 2uf^0(v)f_1^0(v_1) \delta(c) d_c dv_1: \quad (10)$$

Instead of solving (10), the following strategy will be taken. Under the assumption that f is completely known, say by experimental means, we try to find out whether or not (10) is mathematically computable. Seemingly peculiar, this strategy serves us quite well.

The left side can be trivially calculated: at a specified position' $(r;v)$, the side takes a definite and finite value (if there is regularly differentiable). The calculation of the right side is nontrivial: to get a definite value at the same specified position' $(r;v)$ is actually impossible. The basic reason behind the incomputability is that v^0, v_1^0, v, v_1 and c_c are associated with each other rather solidly. Note that v has been specified and $(v^0 + v_1^0)$ points along the v_x axial in this setup; thus v_1 has no choice but to lie on the plane determined by the v_x axial and v (under the momentum conservation law). Similarly, after v and v_1 are specified, there is no degree of freedom for c_c . All these tell us that the integration domain of (10) is just two-dimensional and the integral cannot be calculated (See Appendix A, C and Ref. 1 for more analytical discussions).

In fact, there is no great difficulty to configure other types of setups in which paradoxes concerning Boltzmann's equation show up.

4 Application of the path-integral approach

A sharp and inevitable question arises. What are the true obstacles that keep us from mastering the collective behavior of classical particles while

each of such particles has been formulated for so long? After a long-time effort to find a way out, we come to realize that particles in such system involve a dual nature. Before and after they collide, deterministic path-equations are obeyed; when they collide with boundaries or other particles, indeterminate laws have to be invoked (this is of probability in nature). With the motivation to incorporate path-information into an integral of collision, a new path-integral approach has been proposed [6, 7]. Here, we wish to present a simplified version of it.

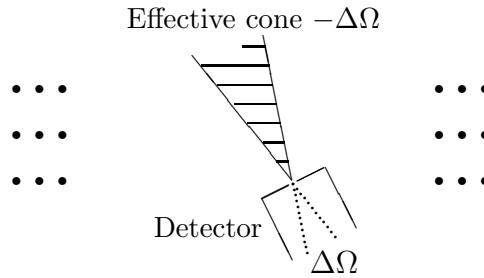


Figure 3: A real or imaginary detector placed at a point where the distribution function is of interest.

The primary concern of the proposed theory is focused on what can be measured in experiments. As in Fig. 3, we consider a particle detector placed at a position where the distribution function needs to be determined. There are key points worth mentioning about the detector.

1. The detector has a really small opening, whose area is denoted by S_0 .
2. Without specifying the concrete structure of the detector, it is assumed that every scattered particle within a specific velocity domain

$$v = v^2 - v^2; \quad (11)$$

will be registered and any others will not. (The central axis of is perpendicular to S_0 .)

3. While S_0 and v are considered to be infinitely small, the domain of , though also small, has been assumed to be finite and fixed. As will be seen, the discrimination against is taken almost entirely from necessity.

If the detector works as described above, do we know the distribution function at the entry of the detector? The answer is basically a positive one. If N is the number that the detector counts during t , the particle density in the phase volume element is

$$f(t; r; v) = \frac{N}{(S_0 v t) (v v^2)}; \quad (12)$$

where r is the position of the detector opening. The form of (12) reveals one of the most distinctive features of this approach: the distribution function is formulated directly. Apart from other merits, this brings a lot of convenience to the verification work.

Examining Fig. 3, we see that only the collisions within the shaded spatial cone, called the effective cone hereafter, can directly contribute to N . Notice that the effective cone is defined with help of path information.

We shall apply the concepts introduced above to our two setups.

4.1 Application to setup 1

Referring to Fig. 1, we wish to determine the distribution function of scattered particles $f(t; r; v)$ under the assumption that the detector opening is at r and there is a piece of the solid surface inside the effective cone.

One of the essential features related to particle-to-boundary collisions is that scattered particles will behave like particles emitted by the surface [5]. In terms of probabilities, the 'emission' rate from a surface element dS^0 , whose position is r^0 , can be defined such that

$$dN = f(t^0; r^0; v^0) dt^0 dS^0 dv^0 d\Omega^0; \quad (13)$$

represents the number of the particles emerging within the solid-angle domain $d\Omega^0$ in the time interval dt^0 and speed range dv^0 . Generally speaking, depends on how the particles are 'sent' to the boundary, how many particles get involved and what kind of boundary exists there. For purposes of this paper, we simply assume that related to each surface element has been known (by experimental means for instance).

The particles 'emitted' from the surface element dS^0 at t^0 will enter the detector opening at t and immediately after getting in they occupy

$$j = r_j^0 + v_j^0 t; \quad (14)$$

where the solid-angle domain Ω_0 is defined as $\Omega_0 = S_0 = j = r_j^0$; and there is a time delay between t^0 and t

$$t = t^0 + j = r_j^0 / v^0; \quad (15)$$

Thus, according to (12), the distribution function at r takes the form

$$f(t; r; v) = \int_{S_0} \int_{r^0}^Z \frac{(t^0; r^0; v^0) dt^0 dS^0 dv^0 d^0}{v^0 dt^0 dv^0 d^0}; \quad (16)$$

where the integration domain S_0 includes all surface elements enclosed by the effective cone (with no blockage assumed). In writing (16), we have used the fact that r^0 is much smaller than r , namely

$$r^0 \ll r; \quad (17)$$

which has been ensured by the fact that the detector opening S_0 is infinitesimal while r is finite. With help of (17), every particle which moves from S_0 and enters the detector will be considered as one whose velocity is in the domain v . We finally arrive at

$$f(t; r; v) = \frac{1}{v^3} \int_{S_0} \frac{(t^0; r^0; v; v^0) dS^0}{\int_{r^0}^Z}; \quad (18)$$

It is easy to see that (18) can be used to calculate the behavior of the scattered particles shown in Fig. 1. However, a much more crucial point is that (18) reveals something that standard approaches have always overlooked: discontinuity almost everywhere. When two adjacent effective cones pertaining to one spatial point contain different boundaries, the velocity distribution there will generally involve discontinuity. In turn, this means that any finite-size boundary will generate discontinuity of velocity distribution at every path-reachable point (collisions along the paths erase such discontinuity partly and gradually though).

4.2 Application to setup 2

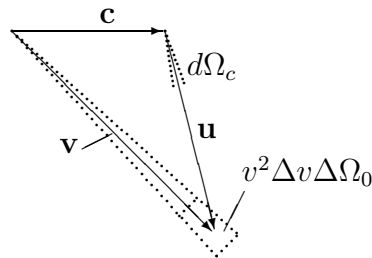
Referring to Fig. 2, we now determine the distribution function of scattered beam 0 particles $f(t; r; v)$, where r is located inside or outside the collision region.

The collisions taking place within dr^0 , where r^0 denotes a spatial point inside the effective cone, can be represented by

$$[2\pi dr^0][f^0(t^0; r^0; v^0) dv^0][f_1^0(t^0; r^0; v_1^0) dv_1^0][(\sigma_c) t^0] d^0; \quad (19)$$

whose derivation can be found in usual textbooks[3]. If the particles produced by the collisions expressed by (19) reach r at the time t , there must be a time delay expressed by $t^0 = t - \int_{r^0}^r \frac{dr}{v}$.

Since this setup is entirely time-independent, time variables will be made implicit in all formulas.



Inserting (1) and (3) into (19) and then integrating (19), we finally obtain, from expression (12),

where $\Omega_0 = S_0 = \mathbf{r}^2$ and the integration domain $(\mathbf{v}; \Omega_0)$ implies that only the particles in \mathbf{v} and in Ω_0 can be taken into account. Again, since Ω_0 holds in most regions inside the effective cone, particles that can enter the detector will be considered as ones within Ω_0 . Based on the notation $c^0 = (v^0 + v_1^0)/2$, $c = (v + v_1)/2$, $u^0 = (v^0 - v_1^0)/2$, $u = (v - v_1)/2$, $c^0 \rightarrow c$, $u^0 \rightarrow u$ and $u^0 \rightarrow u$, the variable transformation from $(v_x^0; v_{1x}^0)$ to $(c^0; u^0)$ and finally to $(c; u)$ is made, and Ω_0 becomes

in which the Jacobian between the variable transformation is

10

By investigating the situation in the velocity space shown in Fig. 4, the following relation can be found out:

$$\int_{v;_0}^Z u^2 d\Omega_c \int_1^{Z-1} du = \frac{1}{2} v v_0 : \quad (23)$$

Therefore, the distribution function at r is

$$f(r; v;) = \frac{4n_0 n_1^0}{v} \int_1^{Z-1} dr^0 \int_1^{Z-1} dc \frac{(\Omega_c) g(c+u) g_1(c-u)}{u r^0 r^0_j}; \quad (24)$$

where Ω_c is the solid angle formed by u and u^0 and u is defined as $u = v(r-r^0) = r-r^0_j - c$.

It is very obvious that (24) is truly calculable and the result is a definite number.

Since Ω_c is a finite solid-angle domain, expression (24) is nothing but the distribution function averaged over Ω_c , which is still different from the 'true and exact distribution function' in the standard theory. However, if we let Ω_c tend to zero, Ω_c will no longer hold and the concept of effective cone will no longer be valid, thus making the whole formalism collapse. A thorough inspection of this approach compels us to believe that the true and exact distribution function is beyond our reach and any attempt to formulate it will ultimately fail.

5 Conclusions

The viewpoints and calculations presented in this paper are waiting to be proved or disproved by real or computational experiments. If they are right, as earnestly expected by us, many fundamental and interesting questions arise. For one thing, this paper hints that differential equations should not be considered as universally effective apparatuses (as many may assume). The following observations are worth mentioning.

In a differential formalism, we either respect path-equations, in which $v = dr/dt$ holds, or respect partial differential equations, in which t, r and v are completely independent. In general, we cannot incorporate path-equations into a partial differential approach.

In view of that the newly-formulated distribution function is an averaged one, the proposed theory is 'approximate' in nature and the time-irreversibility (information loss) has been built in.

According to the proposed theory, the spatial discontinuity associated with a boundary will transform itself into the pervasive velocity discontinuity in the nearby, as well as distant, region. The role that such discontinuity plays in a variety of non-equilibrium phenomena has been overlooked.

For the time being, these observations, as well as many related others, are just matters for conjecture. Reference papers can be found in the regular and e-print literature [6, 7].

Acknowledgment

Communication with Oliver Penrose is gratefully acknowledged. The author also thanks Hanying Guo, Ke Wu and Keying Guan for helpful discussion.

Appendix A : Disproof of Boltzmann's equation

In this appendix, we shall investigate Boltzmann's equation in a brief and direct manner (involving no physical assumptions).

According to the philosophy of standard theory [3], there is an expression characterizing how collisions lessen particles around a specific position r and a specific velocity v

$$\lim_{t; r; v \rightarrow 0} \frac{N_{out}}{t r v}; \quad (25)$$

where N_{out} is the number of the particles that get out of $r v$ during t because of collisions. Likewise, there is an expression characterizing how collisions produce particles around r and v

$$\lim_{t; r; v \rightarrow 0} \frac{N_{in}}{t r v}; \quad (26)$$

where N_{in} is the number of the particles that get in $r v$ during t because of collisions. Although expressions (25) and (26) have served as two of the basic concepts in our understanding to the statistical world (explicitly or implicitly), the recent studies of us fall short of justifying them.

In fact, a paradox associated with (25) can be addressed directly. To calculate expression (25), we are supposed to formulate how many particles initially within $r v$ collide during t and thus leave $r v$. However, if the length scale of r , denoted as j_r , be much smaller than j_v (in the standard theory there is no constraint on how t , r and v tend to

zero), we end up with finding that all the considered particles travel much longer than $j r_j$ during t and almost all the formulated collisions take place outside r . That is to say, in order for (25) to hold its significance, we have no choice but to presume $j r_j \ll j v_j t_j$, which is, unfortunately, in conflict with Boltzmann's equation itself, whose basic conception is that t , r and v are completely independent of each other.

A similar paradox exists concerning (26). To calculate (26), we need to examine how many particles involve collisions inside r during t and acquire velocities within v . However, if $j r_j \ll j v_j t_j$, we find that every examined particle will, after its collision, escape from r in a time much shorter than t and only the particles that collide at the very end of t can be possibly regarded as ones that get in $r \cap v$ during t .

We now turn attention to whether or not (26) is computable (with $j r_j \ll j v_j t_j$ adopted for the discussion hereafter). Consider that the gas of interest consists of many beams and the particles of each beam move at the same velocity. Following the standard methodology, our task is to examine how many beam i particles in r will emerge within the velocity volume element v after colliding with beam j particles. It is easy to see that although the scattering velocities v_i and v_j (of beam i and beam j particles respectively) have all together six components, they are confined to two degrees of freedom since the energy-momentum conservation laws serve as four constraints. Namely, in the velocity space, the ending point of v_i , as well as that of v_j , has to spread over the energy-momentum shell S_{ij} , which is of zero thickness and defined by the initial velocities v_i^0 and v_j^0 (of beam i and j respectively). Then, a serious problem related to (26) is about to surface: the number of the beam i particles emerging within v , labelled as $(N_{in})_{ij}$, cannot be proportional to the volume of v , while $(N_{in})_{ij}$ is trivially proportional to t and r . To this problem, two possible situations are relevant. The first is one in which the shell S_{ij} passes through the convergence point of v (to which v shrinks), and therefore

$$\lim_{t; r; v \rightarrow 0} \frac{(N_{in})_{ij}}{t r v} / \lim_{a \rightarrow 0} \frac{a^2}{a^3} \neq 1; \quad (27)$$

where v has been assumed to be cube-shaped with side length of a and is the local surface density of beam i particles on S_{ij} . The second is one in which S_{ij} does not pass through the convergence point of v , and therefore no beam i particle will emerge within v as $v \rightarrow 0$, i.e.

$$\lim_{t; r; v \rightarrow 0} \frac{(N_{in})_{ij}}{t r v} \neq 0; \quad (28)$$

Expressions (27) and (28) show that the rate (26) is not associated with a definite value even after $j \rightarrow j$ $j \rightarrow j$ $t \rightarrow t$ is adopted. (The manipulation of the standard theory makes the problem less visible, but not absent. See Sect. 3 and Appendix C for more.)

Appendix B : Two types of cross sections

To understand Boltzmann's equation, it is of considerable necessity to know the differences between the cross section in the center-of-mass frame and the cross section in the laboratory frame.

First of all, we examine the collisions between a particle beam (of type 0) and a single particle (of type 1) in the center-of-mass frame. Let Ω_c denote the solid angle formed by the velocity of a scattered type 0 particle with respect to its initial velocity. Then, the cross section $\sigma(\Omega_c)$ is defined such that

$$dN = \sigma(\Omega_c) d\Omega_c \text{ [or } dS_c = \sigma(\Omega_c) d\Omega_c]; \quad (29)$$

represents the number of the scattered type 0 particles emerging within the solid-angle domain $d\Omega_c$ per unit time and per unit relative flux. Since the particles emerging within $d\Omega_c$ actually come from the incident area dS_c , the cross section has the dimension and units of area. As textbooks have clearly elaborated, $\sigma(\Omega_c)$ can be applied normally and easily [2, 3].

Now, we examine the cross section in the laboratory frame. In a seemingly identical way, consider the collisions between a particle beam (of type 0) with velocity v^0 and a single particle (of type 1) with velocity v_1^0 . According to textbooks of statistical mechanics, there is a cross section $\hat{\sigma}$ such that [3]

$$dN = \hat{\sigma}(v^0; v_1^0) |v; v_1| dv dv_1 \quad (30)$$

represents the number of the scattered type 0 particles emerging between v and $v + dv$, while the type 1 particle emerges between v_1 and $v_1 + dv_1$, per unit time and per unit relative flux. At first glance, like $\sigma(\Omega_c)$, $\hat{\sigma}$ in (30) can be applied freely. Our studies, however, reveal that $\hat{\sigma}$ possesses truly misleading features.

As well known, the energy-momentum conservation laws are obeyed in a collision. Assuming all colliding particles to have the same mass (simply for simplicity) and adopting the notation introduced in Sect. 4, we have

$$c = c^0 \quad q_0 \quad \text{and} \quad u = u^0 \quad u_0; \quad (31)$$

where c_0 is the velocity of the center-of-mass and u_0 the speed of particles relative to the center-of-mass. For any specific pair $(v^0; v_1^0)$, c_0 stands for

three constants and u_0 for one, and therefore the degrees of freedom for $(v; v_1)$ are not six but two, as shown in Fig. 5. Namely, in the velocity space, the velocities v and v_1 have no choice but to fall on the spherical shell of radius u_0 , called the energy-momentum shell in this paper. With help of this concept, we concluded in Ref. 1 that scattered particles should be examined with reference to an area element on the energy-momentum shell rather than with reference to a velocity volume element.

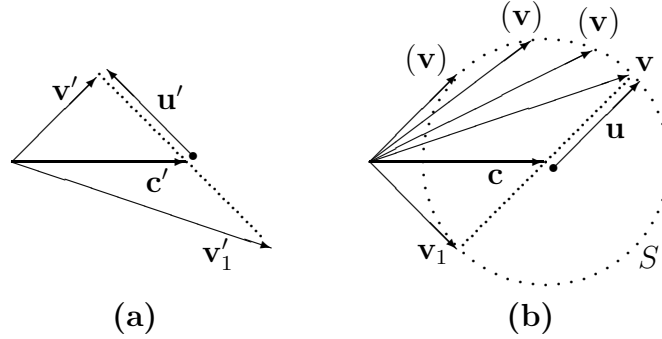


Figure 5: Energy-momentum constraints on scattered particles: (a) v' and v'_1 are the initial velocities, and (b) v and v_1 the final velocities falling on the shell S .

However, some textbooks state that the cross section $\hat{\sigma}$ makes sense in terms of δ -functions[1]. To see whether it is possible and what is meant by it, we rewrite (30) as

$$dN = \hat{\sigma} dv dv_1 = \hat{\sigma} k J k dc du = \hat{\sigma} k J k dc u^2 du d\Omega_c; \quad (32)$$

where $k J k = k \partial(v; v_1) / \partial(c; u) k = 8$ is the Jacobian between the two systems. The comparison between (32) and (29) yields

$$\hat{\sigma}(v^0; v_1^0 | v; v_1) = \frac{1}{u^2 k J k} \delta^3(c - c_0) \delta(u - u_0); \quad (33)$$

where δ^3 is the symbol of three-dimensional δ -function. Obviously, the energy-momentum conservation laws have been included in (33).

Can the cross section $\hat{\sigma}$ so defined offer extra advantages? Or, on second thoughts, can it still cause ill treatments in certain contexts? To answer these questions, we look at Fig. 6, in which two small domains for scattered particles are specified as v and v_1 (initial beam with v^0 and v_1^0 have not been depicted). Under the assumptions that v and v_1 are symmetric

with respect to the center-of-mass and v encloses a small part of the energy-momentum shell, whose area is denoted by S , we obtain, by virtue of (32) and (33),

$$\int_{v; v_1} \hat{g} dv = \int_c \hat{g} dv_c = \int_S \hat{g} dS = u^2; \quad (34)$$

where v_c is associated with v , via $v_c = S/u^2$. Equation (34) illustrates that \hat{g} is essentially defined on the energy-momentum shell S and by the cross section (v_c) .

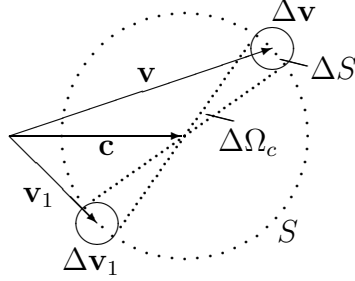


Figure 6: The velocity domains Δv and Δv_1 have to be symmetric with respect to the center of the energy-momentum shell.

If there exists no explicit constraint on v and v_1 (other than the energy-momentum conservation laws), expression (34) becomes

$$\int_{v, v_1} \hat{g} dv = \int_c \hat{g} dv_c; \quad (35)$$

where the subindex (4) of the last integral means that the integral is over the entire domain of v_c .

If v encloses a small part of the energy-momentum shell $S = u^2 v_c$ while v_1 is subject to no explicit constraint, then the expression

$$\int_{v, v_1} \hat{g} dv \quad (36)$$

seems to differ from (34) in an obvious way. However, the difference is a misleading one. Due to the existence of energy-momentum conservation laws, the components of v and v_1 are intrinsically connected, and therefore (36) yields exactly the same result as (34) does.

In Appendix C, it will be unveiled that, associated with mistreating (36), the standard formalism involves a mathematical error.

Appendix C : A n error in the textbook treatment

According to textbooks, the regular Boltzmann equation is based on [3]

$$\frac{\partial f}{\partial t} + \mathbf{v} \cdot \frac{\partial f}{\partial \mathbf{r}} + \frac{\mathbf{F}}{m} \cdot \frac{\partial f}{\partial \mathbf{v}} = \lim_{t \rightarrow \infty} \frac{(\dot{N})_{in} - (\dot{N})_{out}}{t}; \quad (37)$$

where $(\dot{N})_{in}$ and $(\dot{N})_{out}$ stand for the particles that enter and leave $\mathbf{r} \cdot \mathbf{v}$ during t due to collisions. In this appendix, we ignore the paradoxes unveiled in Appendix A and concern ourselves solely with how textbooks treat (37) in the mathematical sense.

The textbook methodology of formulating $(\dot{N})_{out}$ is that, for a definite \mathbf{r} , the particles leaving \mathbf{v} during t due to collisions are identified as $(\dot{N})_{out}$. On this understanding, $f_1(\mathbf{v}_1)d\mathbf{v}_1$ represents the particles knocking some particles out of the beam $f(\mathbf{v})d\mathbf{v}$, and we get

$$(\dot{N})_{out} = \int_{\mathbf{v}, \mathbf{v}_1, \mathbf{v}_1^0}^Z 2u_r [f(\mathbf{v})d\mathbf{v}] [f_1(\mathbf{v}_1)d\mathbf{v}_1] [\hat{\sigma}(\mathbf{v}, \mathbf{v}_1; \mathbf{v}^0, \mathbf{v}_1^0)] d\mathbf{v}^0 d\mathbf{v}_1^0; \quad (38)$$

where $\hat{\sigma} = \hat{\sigma}(\mathbf{v}; \mathbf{v}_1; \mathbf{v}^0; \mathbf{v}_1^0)$ is the cross section in the laboratory frame. With help of (35), we get

$$\lim_{t \rightarrow \infty} \frac{(\dot{N})_{out}}{t} = \int_{\mathbf{v}_1; c(4)}^Z 2u_r (\dot{N})_{out} = \int_{\mathbf{v}_1; c(4)}^Z 2u_r (\dot{N})_{out} f(\mathbf{v}) f_1(\mathbf{v}_1) d\mathbf{v}_1 d\mathbf{v}_c; \quad (39)$$

where \mathbf{v}_1 is unlimited and the domain of \mathbf{v}_c is (4). So far, every thing is exactly the same as that in the textbook treatment.

A similar methodology is employed to formulate $(\dot{N})_{in}$. $f^0(\mathbf{v}^0)d\mathbf{v}^0$ and $f_1^0(\mathbf{v}_1^0)d\mathbf{v}_1^0$ are identified as two colliding beams, and we have

$$(\dot{N})_{in} = \int_{\mathbf{v}^0, \mathbf{v}_1^0; \mathbf{v}, \mathbf{v}_1}^Z 2u_r [f^0(\mathbf{v}^0)d\mathbf{v}^0] [f_1^0(\mathbf{v}_1^0)d\mathbf{v}_1^0] [\hat{\sigma}(\mathbf{v}^0, \mathbf{v}_1^0; \mathbf{v}, \mathbf{v}_1)] d\mathbf{v} d\mathbf{v}_1; \quad (40)$$

where $\hat{\sigma} = \hat{\sigma}(\mathbf{v}^0; \mathbf{v}_1^0; \mathbf{v}; \mathbf{v}_1)$ and \mathbf{v} is used to remind us that only the particles emerging within \mathbf{v} will be taken into account. Although the symmetry between (38) and (40) appears obvious and has played a vital role in deriving the Boltzmann equation, we are now convinced that it is an illusive one. Due to the existence of the energy-momentum conservation laws, when \mathbf{v} in (40) is limited to an infinitesimal volume \mathbf{v} , \mathbf{v}_1 must be

limited to the symmetric v_1 , while v_1 in (39) is unlimited. That is to say, (40) should be replaced by

$$(\bar{N})_{in} = \int_{v_1^0; v_1}^Z [u(r)] [f^0(v^0) dv^0] [f_1^0(v_1^0) dv_1^0] [\wedge t] dv dv_1: \quad (41)$$

So, the aforementioned symmetry disappears and we arrive at

$$\lim_{t \rightarrow v \neq 0} \frac{(\bar{N})_{in}}{t r v} \notin \int_{v_1; c(4)}^Z 2u(r) f^0(v^0) f_1^0(v_1^0) dv_1 dv: \quad (42)$$

As Appendix A has shown, a serious evaluation of the left side of (42) actually leads us to nowhere.

References

- [1] C. Y. Chen, Il Nuovo Cimento B V 117B, 177-181 (2002).
- [2] L. D. Landau and E. M. Lifshitz, Mechanics, (Pergamon Press, 1976).
- [3] See, for instance, F. Reif, Fundamentals of Statistical and Thermal Physics, (McGraw-Hill Book Company, 1965, 1987, 1988 in English and German). This is a textbook for students, so it offers the most elementary and detailed illustration of how Boltzmann's equation is derived.
- [4] R. Kubo, M. Toda and N. Hashitsume Statistical Physics II, 2nd Ed., (Springer-Verlag, 1995).
- [5] See, for instance, M. N. Kogan Rarefied Gas Dynamics, (Plenum Press, New York, 1969).
- [6] C. Y. Chen, Perturbation Methods and Statistical Theories, in English, (International Academic Publishers, Beijing, 1999).
- [7] C. Y. Chen, cond-mat/0504497, 0412396; physics/0312043, 0311120, 0305006, 0010015, 0006033, 0006009, 9908062; quant-ph/0009023, 0009015, 9911064, 9907058.